JOURNAL OF MATERIALS SCIENCE 26 (1991) 2557–2565

Organo-inorganic composite membranes: a mathematical modelling approach to the solid–liquid interaction properties of asbestos in its composites

L. PELLEGRINI, E. MONTONERI*
Dipartimento di Chimica Industriale ed Ingegneria Chimica Giulio Natta, Politecnico di Milano, P. zza L. da Vinci 32, 20133 Milano, Italy

P. SAVARINO
Dipartimento di Chimica Generale ed Organica Applicata, Università di Torino, Corso Massimo D'Azeglio n.48, 10125 Torino, Italy

G. C. PAPPALARDO
II Cattedra di Chimica Generale, Facoltà di Farmacia, Dipartimento di Scienze Chimiche dell'Università di Catania, V. le A. Doria 8, 95125 Catania, Italy

Data for the liquid sorption (Y) by asbestos membranes, coated with polyphenylene sulphide or with polyphenylene sulphide sulphonic acid and having variable polymer concentration (X) and acid equivalent (EW) values, have been fitted by multivariable mathematical models relating Y to X and EW in the bulk and in the surface membrane phase. The results point out that (i) the membrane surface is the sorption-limiting phase at low porosity, (ii) under this condition the liquid sorption selectivity depends on the membrane acid equivalent concentration, and (iii) the membrane acid functions allow both macro-permeation, into the bulk phase, and micro-permeation, through the coating layer into the asbestos support structure, of aqueous media.

1. Introduction

A subject of interest in membrane studies is the evaluation of the single contributions of the membrane physical structure and of the chemical nature to its performance. In an organo-inorganic composite membrane, both these parameters can be varied over a wide range upon changing the concentration ratio of the constituents. Asbestos coated with organic polymers is a typical example of this situation. In the composites manufactured by soaking asbestos paper with a polymer solution and drying [1], the polymer is deposited over the asbestos fibres and, as the thickness of the coating layer grows by increasing the concentration of the polymer in the soaking bath, the material void fraction decreases. At the same time, as the concentration ratio of the lipophilic organic polymer to the hydrophilic inorganic material increases, the chemical interaction between the solid phase and the external phase is subject to substantial changes. This manufacturing technique has also been found [2] to yield higher polymer concentration on the membrane surface faces than in the bulk of the solid phase. Therefore, both the physical structure and the chemical nature of the membrane change throughout the membrane phase. In addition to their importance as cell separators [3, 4] for alkaline water electrolysis and electrochemical chlor-alkali production, these composites offer scope for investigating the role of the membrane's physical and chemical features and of the bulk and surface membrane phases in solid–liquid interactions.

In a previous work on asbestos coated with polyphenylene sulphide (PPS), a quantitative evaluation [5] of the relative contributions of the above parameters to the membrane performance was attempted, based on the study of the sorption of chemically different liquids by the solid material and on a stepwise multivariable regression analysis of the experimental data. The results pointed out that, whereas water sorption is strongly dependent on the concentration of the organic polymer upon the membrane surface, the sorption of toluene is not affected by this parameter. It has therefore been suggested that, at low membrane porosity, liquid sorption by the solid phase is ruled mainly by the solid–liquid chemical interactions and that the liquid sorption selectivity should be largely governed by the chemical nature of the membrane surface phase.

This work aimed to provide experimental support for the above indications and to investigate how the

* Author to whom all correspondence should be addressed.

0022–2461/91 $03.00 + .12

change in the polymer nature, from the lipophilic state, as in PPS, to the more hydrophilic state, as in sulphonated polyphenylene sulphide (SPPS) [6], affects the membrane surface behaviour. Thus, the previous approach [5] used to study asbestos coated with PPS has now been extended to the study of asbestos coated with SPPS. Three types of sulphonated polymer were used to coat asbestos; these differ in the concentration of acid equivalents (PAE = 1.40, 0.769 and 0.625 H^+ meq/g polymer). The change in the type and concentration of the polymer in the composite membrane provided a large number of samples having a range of membrane acid equivalents (EW) from 0–6.4 $\times$ 10^{-4} H^+ eq/membrane g, distributed in the bulk and surface phase of the composite membrane. Several multivariable mathematical models relating liquid sorption with the membrane polymer concentration and with the membrane acid equivalents, both in the bulk and surface phases, have been tested to fit the experimental data. The previous models [2] tested for asbestos coated with PPS did not account for the change in the polymer nature as given by the EW parameter.

2. Experimental procedure

The manufacture of the asbestos–PPS (ASB–PPS) composites from commercial crysotile asbestos (ASB) paper (0.55 mm thick) and polyphenylene sulphide, and of the asbestos–SPPS (ASB–SPPS) composites from ASB and polyphenylene sulphide sulphonic acid (SPPS) was accomplished as previously reported [2, 6]. The polymer concentrations (% wt/wt) in the bulk (X_1) and in the surface (X_2) phases of the membrane and the total polymer concentration (P) and brucite (B) concentration have been determined by infrared spectroscopy [2]. The acid equivalent concentration of the neat organic polymer (PAE = SO_3H eq/g polymer) was obtained by titration with 0.1 N NaOH. The acid equivalent concentration of the composite material (EW = SO_3H eq/g composite) in the bulk (EW_1) and in the surface (EW_2)

TABLE I Polymer (X_n, % wt/wt) and membrane acid equivalent (EW_n, H^+ eq/g membrane) concentrations in the bulk (n = 1) and surface (n = 2) phases of fresh asbestos composites versus sorption (Y_i, ml/g dry membrane) of water (i = H) and of toluene (i = t)

X_1	EW_1($\times$ 10^4)	X_2	EW_2($\times$ 10^4)	Y_H	Y_t	Y_H/Y_t
0.0	0.00	0.0	0.00	0.440	0.439	1.002
8.9	0.00	23.3	0.00	0.399	0.439	0.909
8.9	0.00	23.3	0.00	0.389	0.455	0.855
11.3	0.00	18.9	0.00	0.330	0.366	0.902
11.3	0.00	18.9	0.00	0.330	0.379	0.871
16.5	0.00	19.9	0.00	0.317	0.350	0.906
16.5	0.00	19.9	0.00	0.344	0.358	0.961
17.1	0.00	36.5	0.00	0.195	0.337	0.579
21.6	0.00	27.3	0.00	0.198	0.290	0.683
21.6	0.00	27.3	0.00	0.153	0.270	0.567
21.5	0.00	52.7	0.00	0.117	0.296	0.395
29.4	0.00	60.4	0.00	0.090	0.195	0.462
29.4	0.00	60.4	0.00	0.083	0.194	0.428
28.9	0.00	52.7	0.00	0.129	0.207	0.623
52.4	0.00	68.1	0.00	0.041	0.079	0.519
52.4	0.00	68.1	0.00	0.071	0.116	0.612
51.5	0.00	80.9	0.00	0.069	0.095	0.726
41.3	5.16	51.1	6.39	0.150	0.180	0.833
28.3	1.77	40.2	2.52	0.220	0.320	0.688
28.3	1.77	40.2	2.52	0.230	0.330	0.697
26.1	2.01	35.5	2.73	0.220	0.430	0.512
26.1	2.01	35.5	2.73	0.210	0.410	0.512
24.0	1.84	33.5	2.58	0.230	0.380	0.605
24.0	1.84	33.5	2.58	0.180	0.400	0.450
24.6	1.89	45.9	3.53	0.190	0.410	0.463
24.6	1.89	45.9	3.53	0.240	0.390	0.615
21.2	2.97	31.8	4.45	0.230	0.430	0.535
21.2	2.97	31.8	4.45	0.170	0.460	0.370
16.9	2.37	39.6	5.55	0.230	0.450	0.511
16.9	2.37	39.6	5.55	0.180	0.470	0.383
8.1	1.14	22.9	3.21	0.210	0.480	0.438
8.1	1.14	22.9	3.21	0.210	0.470	0.447
25.5	1.59	36.9	2.31	0.180	0.430	0.419
27.5	1.72	45.9	2.87	0.170	0.430	0.395
22.2	1.39	36.7	2.29	0.180	0.230	0.783
25.0	1.93	40.5	3.11	0.210	0.380	0.553
25.5	1.59	36.9	2.31		0.410	
27.5	1.72	45.9	2.87		0.360	
25.0	1.93	40.5	3.11	0.180		
22.2	1.39	36.7	2.29	0.250	0.390	0.641

phases was calculated as follows: $EW_1 = PAE\,X_1/100$ and $EW_2 = PAE\ X_2/100$. All other experimental details are as previously published [2].

3. Results and discussion

3.1. The chemical and physical nature of the composites

There are two sets of samples in this work. The first set (Table I) contains materials as-made, the second set (Table II) contains the same materials which were aged in 30% boiling KOH for 2500 h in order to test the chemical stability of asbestos as a function of the coating polymer. SEM studies have shown that, whereas in the fresh materials the membrane porosity is directly related to the concentration of the organic polymer, no such relationship appears in the aged materials. The composites, particularly those containing SPPS, undergo weight loss in alkali. This phenomenon is mainly due to the degradation of asbestos by the alkali and to leaching of soluble silicon into the aqueous phase [2]

$$Mg_3Si_2O_5(OH)_4 + 2\,KOH = 3\,Mg(OH)_2 + \text{soluble silicates(aq)} \quad (1)$$

rather than to the loss of the organic polymer. Table II shows that the polymer concentration in the aged composites, relative to that in the fresh material, does not change much. The most significant change is the presence of brucite and, therefore, a decrease in the concentration of asbestos. Infrared spectroscopy showed that the weight loss (*cwl*), calculated [2] from the material compositional change and by assuming that the weight loss is due to the loss of silicon as in Reaction 1, is statistically not different from nor accounts for most of the material loss (*twl*) determined by weighing. The consequences of the degradation involve both chemical and morphological changes in the composites, as compared to the corresponding

TABLE II Polymer (P, % wt/wt), brucite (B, % wt/wt), acid equivalent (EW, H^+ eq/g membrane) concentration, calculated ($cwl \pm 2.2$, % wt/wt) and experimental ($twl \pm 2.0$, % wt/wt) weight loss and sorption (Y_i, ml/g dry membrane) of water (i = H) and toluene (i = t) for asbestos composites aged (a) 2500 h in 30% boiling KOH versus polymer (X_1, % wt/wt) and acid equivalent concentration (EW_1, H^+ eq/g membrane) in the material (f)

f		a								
X_1	$EW_1(\times 10^4)$	S[b]	P	$EW(\times 10^4)$	B	cwl	twl	Y_H[a]	Y_t[a]	Y_H/Y_t
0.0	0.00	b	0.0	0.00	61.4	40.3	32.2	0.860	0.681	1.26
		s	0.0	0.00	61.4	40.3				
8.9	0.00	b	18.6	0.00	7.1	7.4	14.0	0.696	0.686	1.01
		s	32.5	0.00	3.1	4.0				
13.4	0.00	b	12.4	0.00	9.0	8.6	9.3	0.710	0.699	1.02
		s	32.9	0.00	8.7	10.8				
16.9	0.00	b	23.4	0.00	7.6	8.4	7.9	0.553	0.542	1.02
		s	6.9	0.00	8.2	7.4				
17.1	0.00	b	20.7	0.00	8.9	9.5	6.5	0.516	0.511	1.01
		s	35.9	0.00	7.3	9.5				
20.1	0.00	b	27.6	0.00	4.7	5.6	11.1	0.422	0.424	0.99
		s	31.0	0.00	6.0	7.3				
22.7	0.00	b	34.7	0.00	7.2	9.2	8.3	0.300	0.289	1.04
		s	44.2	0.00	3.6	5.5				
22.7	0.00	b	26.1	0.00	9.9	11.1	12.1	0.450	0.405	1.11
		s	38.4	0.00	6.6	9.0				
24.9	0.00	b	39.8	0.00	4.1	5.8	5.6	0.200	0.225	0.89
		s	41.5	0.00	3.3	4.9				
50.5	0.00	b	44.4	0.00	1.6	2.6	4.2	0.102	0.118	0.86
		s	69.6	0.00	0.0	0.0				
54.1	0.00	b	50.4	0.00	0.0	0.0	0.9	0.101	0.116	0.87
		s	53.9	0.00	0.0	0.0				
14.9	2.09	b	4.6	0.64	41.5	20.2	28.9	1.09	0.930	1.17
		s	27.0	3.78	27.1	17.8				
17.2	1.32	b	27.1	2.13	29.2	19.1	27.1	0.850	0.820	1.04
		s	33.5	2.58	27.4	19.4				
17.2	2.41	b	15.2	2.14	69.5	32.4	36.6	1.07	0.970	1.10
		s	2.0	0.27	74.8	30.8				
22.5	1.41	b	25.9	1.60	5.4	4.1	13.9	0.580	0.580	1.00
		s	43.1	2.69	3.2	3.2				
25.0	1.56	b	26.2	1.64	29.1	18.7	26.8	0.920	0.950	0.97
		s	51.6	3.23	16.7	16.8				
27.2	2.10	b	20.7	1.60	46.0	25.3	36.8	0.860	0.850	1.01
		s	37.8	2.68	36.9	24.8				
29.6	1.85	b	32.4	2.48	57.8	33.2	37.6	1.26	1.26	1.00
		s	43.8	3.37	46.2	32.4				
31.8	1.99	b	35.2	2.20	31.4	22.0	25.9	1.00	0.930	1.07
		s	13.5	0.84	32.3	19.3				

[a] averages of duplicates; [b] bulk (b) and surface (s) samples (S).

initial material. Because of the formation of brucite, the aged materials are tricomposite materials which contain unconverted asbestos, brucite and the organic polymer. Thus, in the aged material the type of chemical interaction with the external liquid phase is expected to change relative to the initial material. Also, because of the loss of silicon, the void volume of the initial material increases in the aged material and this also causes a change in the solid–liquid physical interaction. Degradation indeed involves a change in the initial microstructure, where asbestos is the mechanical support component [2], into one where the organic polymer seems to work as a binding agent [7] for the brucite particles formed. For the scope of this work, the fresh and aged materials have therefore been treated as separate sets.

3.2. Liquid sorption

Liquid sorption may occur by physical entrapment of the liquid into the void volume of the solid phase and/or by chemisorption. Thus the total amount of sorbed liquid (Y) is given by $Y = Y_{ph} + Y_{ch}$, where Y_{ph} is the volume of physisorbed liquid and Y_{ch} is the volume of chemisorbed liquid which is bound to the solid phase by ionic, polar or Van der Waals interactions. For the fresh materials, the volume of sorbed liquid (Y, ml/g dry solid) has been assumed to change with the concentration (X, % wt/wt) of organic polymer in the solid phase as in

$$Y = V_0 - X/(100\,d) + s_0(100 - X)/100 + s_1 X/100 \quad (2)$$

where V_0 (ml g^{-1}) is the void volume of uncoated asbestos, d (ml g^{-1}) is the density of the solid coating polymer, s (ml g^{-1}) is the specific volume of chemisorbed liquid by the asbestos phase (s_0) or by the polymer phase (s_1), X and 100-X are the concentrations (% wt/wt) of the polymer and of asbestos, respectively, as defined in Section 2. In Equation 2, $X/100\,d$ is the specific volume occupied by the polymer phase. Thus $V_0 - X/(100\,d) = Y_{ph}$ and the sum of the terms preceded by the coefficient s represents the total specific volume of chemisorbed liquid (Y_{ch}). If no chemical solvation interaction occurs between the solid and the liquid, $s = 0$ and Y should not depend on the nature of the liquid, but only on the sorbing material. Where chemical interactions occur, s (and therefore Y) depends on the nature of the liquid and of the solid. The porous neat asbestos which has been used in this work absorbs equal volumes of liquids which differ greatly in polarity (Table I). It may be assumed, therefore, that due to the high porosity, $Y_{ph} \gg Y_{ch}$ and, therefore, $V_0 \gg s_0\,(100 - X)/100$. Thus, Equation 2 is approximated to

$$Y = V_0 - X/(100\,d) + s_1 X/100 \quad (3)$$

The experimental data (Table I) show, however, that for the composites, the volume of sorbed water (Y_{ph}) and that of sorbed toluene (Y_t) are not equal; therefore the relative contribution (Y_{ch}/Y) of chemisorption to the total liquid sorption cannot be neglected. Equation 2 predicts that this contribution is expected to grow as the solid phase porosity (Y_{ph}) decreases.

In the case of membranes, in order for the liquid to occupy the whole void volume in the solid phase, diffusion through the surface into the bulk phase is necessary. If the surface is not porous, diffusion may occur only by a chemical mechanism; it requires that the liquid is soluble in the surface phase and that chemical exchange of solute molecules occurs between the surface and the bulk phase. If the coefficient s for a given solid–liquid system is small or nil, the total liquid sorption by the membrane may be far lower than that expected by the total membrane void volume, even if this is large because the bulk phase is very porous. Because the materials of this work present such a morphological difference between the bulk and the surface phase, we have assumed the following modified form for Equation 3

$$Y = V_0 - X_1/(100\,d) + s_1 X_1/100 - X_2/(100\,d) + s_1 X_2/100 \quad (4)$$

where the physical and chemical contributions of the bulk and surface phases are represented by the respective X_1 and X_2 polymer concentration terms.

It may be observed that the composite membranes in Table I may be grouped in two categories, apolar or lipophilic (ASB–PPS, $EW = 0$) and polar or hydrophilic (ASB–SPPS, $EW > 0$). For each category, the sorption of a polar (water) and of an apolar (toluene) liquid has been studied. The change of the coefficients d and s in Equation 4, due to the change of the liquid and the polymer nature, is not known. Also the concentration variables X_1 and X_2 in Table I do not identify the chemical nature of the solid phase, whereas the variables EW_1 and EW_2 do.

In order to relate the water (Y_H) and the toluene (Y_t) sorption to the materials' measured variables, we have analysed several model equations which are based on the additivity principle of Equations 2–4 and contain the X and EW variables and the constants B and A_n, $1 \leq {}_n \leq {}_{10}$

$$Y_H = Y_{Ha} + Y_{Hb} \quad (5)$$

where

$$Y_{Ha} = B + A_1 X_1 + A_2 X_2 + A_3/(1 + X_1)^2 + A_4 X_1 X_2 \quad (6)$$

and

$$Y_{Hb} = A_5 EW_2^3 + A_6 EW_2^2 + A_7 EW_2 X_2 + A_8 EW_1^3 + A_9 EW_1^2 + A_{10} EW_1 \quad (7)$$

or

$$Y_{Hb} = A_5(EW_2 + 1)^3 + A_6(EW_2 + 1)^2 + A_7 EW_2 X_2 \quad (8)$$

$$Y_t = B + A_1 X_1 + A_2 X_1^2 + A_3/(1 + X_1) + A_4/(1 + X_1)^2 + A_5 EW_1^3 + A_6/(1 + EW_1) + A_7 EW_2 X_1 + A_8 EW_2^3 + A_9/(1 + EW_2) + A_{10} EW_1 X_1 \quad (9)$$

$$Y_t = B + A_1X_1 + A_2X_1^2 + A_3/(1 + X_1) + A_4/(1 + X_1)^2 + A_5EW_1^3 + A_6EW_1^2 + A_7EW_1 + A_8EW_2^3 + A_9EW_2^2 + A_{10}EW_2^2X_1 \quad (10)$$

$$Y_t = B + A_1X_1 + A_2X_1^2 + A_3/(1 + X_1) + A_4/(1 + X_1)^2 + A_5/(1 + X_1)^3 + A_6EW_1^3 + A_7EW_1^2 + A_8EW_1 + A_9EW_1X_1 \quad (11)$$

These models contain more terms than Equation 4. The additional terms have been arbitrarily introduced in the attempt to find any dependence of d and s on the membrane chemical composition, because this dependence is not defined in Equation 4. The evaluation of the degree of fitting of models 5–11 with experimental data is performed here by stepwise elimination of one least-significant parameter per run (Tables III and IV), starting with the full model. The

TABLE III Stepwise regression analysis of models 5–8 with Table I water sorption data

Run	Model	Tsd. and sign. coeff.[a]										ρ[b]	E[c]	F[d]
		A_1	A_2	A_3	A_4	A_5	A_6	A_7	A_8	A_9	A_{10}			
1	5, 6, 7[e]	a	a	a	a	a	a	c	a	b	d	0.957	0.9663	2.65
2		a	a	a	a	a	a	a	a	a		0.956	0.9601	2.64
3		a	a		a	a	a	a	b	b		0.930	1.4622	4.02
4		a	a		a	b	a	a	d			0.912	1.7443	4.79
5		a	a		a	b	a	a				0.910	1.7283	4.75
6		b	a		a		b	b				0.889	2.0377	5.60
7		c	a		c			d				0.873	2.2487	6.18
8		c	a		c							0.872	2.2009	6.04
9			a		d							0.857	2.3613	6.69
10			a									0.854	2.3472	6.45
11	5, 6, 8[f]	a	a	d	a	a	d	a				0.917	1.6615	4.56
12		a	a	d	b	a		a				0.913	1.6703	4.59
13		b	a		b	a		a				0.908	1.7131	4.71

[a] Tested coefficient with F-test significance $< 90\%$ (d), $\geq 90\%$ (c), $\geq 95\%$ (b), $\geq 99\%$ (a).
[b] Correlation coefficient.
[c] 10^3 MSE; MSE (residual mean square error).
[d] $F = MSE/\sigma_{ex}^2$; σ_{ex}^2 (pooled variance from Y_H duplicate measurements) $= 0.3640 \times 10^{-3}$; 99% confidence level value from F-Tables at 37 and 15 degrees of freedom = 3.15.
[e] Using model 5, where Y_{Ha} is given by Equation 6 and Y_{Hb} is given by Equation 7 in runs 1–10.
[f] Using model 5, where Y_{Ha} is given by Equation 6 and Y_{Hb} is given by Equation 8 in runs 11–13.

TABLE IV Stepwise regression analysis of models of 9–11 with Table I toluene sorption data[a]

Run	Model	Tsd. and sign. coeff.										ρ	E	F
		A_1	A_2	A_3	A_4	A_5	A_6	A_7	A_8	A_9	A_{10}			
1	9[b]	d	d	d	d	b	d	d	d	d	d	0.9531	1.5513	2.77
2	9[b]	d	d	d	d	a	b	d	d	d		0.9531	1.4959	2.67
3	9[b]	a		a	a	a	a	d	d	b		0.9526	1.4576	2.60
4	9[b]	a		b	b	a	a		d	d		0.9491	1.5119	2.70
5	9[b]	a		b	b	a	a			d		0.9460	1.5480	2.76
6	9[b]	a		b	b	a	a					0.9432	1.5756	2.81
7	9[b]	a			d	a	a					0.9371	1.6874	3.01
8	9[b]	a				a	a					0.9367	1.6468	2.94
9	9[b]	a					a					0.8770	3.0149	5.38
10	9[b]	a										0.7773	5.0251	8.97
11	10[c]	d	d	d	d	b	c	d	d	d	c	0.9549	1.4936	2.67
12	10[c]	a		a	a	a	b	d	d	d	c	0.9546	1.4466	2.62
13	10[c]	a		a	a	a	a		d	d	b	0.9541	1.4130	2.52
14	10[c]	a		a	a	a	a			d	b	0.9519	1.4299	2.55
15	10[c]	a		a	a	a	a				c	0.9480	1.4922	2.66
16	10[c]	a		b	b	a	a					0.9420	1.6083	2.87
17	10[c]	a			d	a	a					0.9335	1.7795	3.18
18	10[c]	a				a	a					0.9329	1.7431	3.11
19	10[c]	a					b					0.8045	4.6064	8.22
20	11[d]	d	d	d	d	d	a	b	d	d		0.9580	1.3413	2.39
21	11[d]	c	d		d	d	a	b	d	a		0.9569	1.3289	2.37
22	11[d]	a	a			a	a	b	d	a		0.9563	1.3014	2.32
23	11[d]	a	a			b	a	a		a		0.9541	1.3232	2.36
24	11[d]	a	c				a	a		b		0.9450	1.5283	2.73
25	11[d]	a					a	a		d		0.9380	1.6648	2.97

[a] All symbols and abbreviations as in Table III; $\sigma_{ex}^2 = 0.5603 \times 10^{-3}$.
[b] Used in runs 1–10.
[c] Used in runs 11–19.
[d] Used in runs 20–25.

choice of the best fitting equation is based on several criteria [8, 9]: the value of the correlation coefficient (ρ), the significance level of the A constants and the significance of the residual mean square error of the correlation (MSE) relative to the variance (σ^2_{ex}) of the experimental Y_H measurements as obtained from the pool of each duplicate measurement variance.

For water sorption, the MSE/σ^2_{ex} variance test shows that, for the equations tested in runs 1 and 2, this ratio is lower than the statistical $F_{0.01}$ tabulated value. It can therefore be assessed, with over 99% probability of not being wrong, that the MSE value is not significantly higher than σ^2_{ex} and that these equations are correct models, with that in run 2 (Equation 2–III i.e. run 2, Table III–see Table V) containing constants that are all significantly more than zero from the statistical point of view. The other equations do not seem to account as well for the variability of Y_H in excess of the experimental error. It may be observed that among the EW terms, the EW_2 terms are more significant than the EW_1 ones, these latter being eliminated first. Other models (not shown), which contain all or part of the other EW terms in the models 5–8 multiplied by X_2 or by X_1, were definitely worse than those shown in Table III.

For toluene sorption, all equations tested in Table IV appear correct based on the MSE/σ^2_{ex} criterion, except those in runs 9, 10, 17, 18 and 19. There are four equations (i.e. those in run 6, 8, 16 and 23) which pass all three statistical tests as follows: $\rho > 0.90$, MSE/σ^2_{ex} < statistical $F_{0.01}$ tabulated value at $> 99\%$ confidence level, and the parameters significance level $> 95\%$. These equations, contrary to the water sorption equations in Table III, contain only bulk parameters.

For the most significant equations of Tables III and IV, the values of the constants are given in Table V. It can be observed that one same variable appears often more than once in the same equation and exhibits at the same time a positive and a negative effect on Y, according to the theoretical expectations.

Owing to their empirical nature, the values of the constants in Table V are strictly valid in the experimental ranges ($0 \leq X$ (%) ≤ 80, $0 \leq EW$ (meq g^{-1}) ≤ 0.64) and for the experimental X–EW sets of values. Therefore, extrapolations of the above equations to X and EW values which are far out of the experimental range may yield unreal predictions. The results appear consistent with the expectation (Equations 2, 3 and 4) that, as porosity decreases, the relative contribution of chemical solvation interactions to the total membrane liquid sorption increases, and that as the contribution of chemical sorption increases, the membrane surface acquires a dominant role in determining liquid sorption selectivity. Water sorption on ASB–PPS may be assumed to occur mainly by a physical mechanism due to the low solubility in the PPS coating phase [5]. Thus the membrane surface is expected to be the sorption-limiting phase. The plot of Equation 2–III (i.e. that of run 2 in Table III) at $EW_1 = EW_2 = 0$ shows indeed (Fig. 1) a strong sorption-inhibiting effect from the membrane surface polymer concentration. For toluene sorption, on the other hand, the PPS surface concentration does not need to be considered. The previous work performed on ASB–PPS membranes only [5] showed indeed that a model containing the surface concentration may also fit the toluene sorption experimental data, but the predicted effect is quantitatively negligible. The results here indicate that the highest sorption selectivity is achieved with membranes having very porous bulk phase and a non-porous surface phase. For an ASB–PPS membrane ($EW_1 = EW_2 = 0$) with porous bulk phase ($X_1 = 10\%$), Fig. 2 shows the effect of the

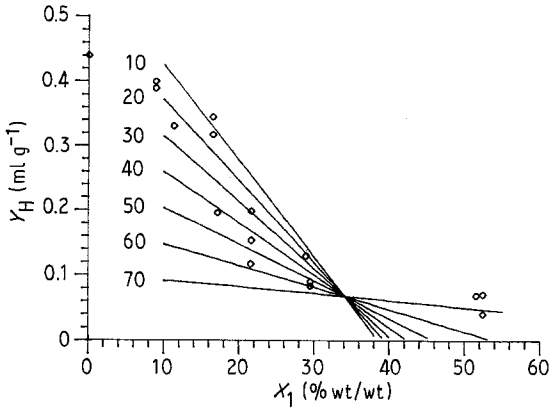

Figure 1 Water sorption (Y_H, ml g^{-1}) versus bulk polymer concentration (X_1, % wt/wt): Y_H calculated from Equation 2–III for $EW_i = 0$ at constant surface polymer concentration (X_2, % wt/wt, number next to each solid line); (○) experimental points.

TABLE V Values of the constants in the best fitting equations (i–n)[a] of Tables III and IV

	Equation (i–n)	
	2–III	23–IV
B	0.657	0.559
A_1	$-(1.73 \pm 0.27) \times 10^{-2}$	$-(1.60 \pm 0.27) \times 10^{-2}$
A_2	$-(7.91 \pm 1.06) \times 10^{-3}$	$(1.36 \pm 0.43) \times 10^{-4}$
A_3	$-(2.16 \pm 0.54) \times 10^{-1}$	
A_4	$(2.32 \pm 0.38) \times 10^{-5}$	
A_5	$(6.57 \pm 1.12) \times 10^{9}$	$-(1.20 \pm 0.49) \times 10^{-1}$
A_6	$-(5.82 \pm 0.88) \times 10^{6}$	$-(8.51 \pm 1.18) \times 10^{9}$
A_7	$(2.06 \pm 0.33) \times 10$	$(2.79 \pm 0.90) \times 10^{6}$
A_8	$-(1.25 \pm 0.26) \times 10^{10}$	
A_9	$(6.87 \pm 1.49) \times 10^{6}$	$(2.23 \pm 0.72) \times 10$

[a] Identified by the run number (i) followed by the table number (n).

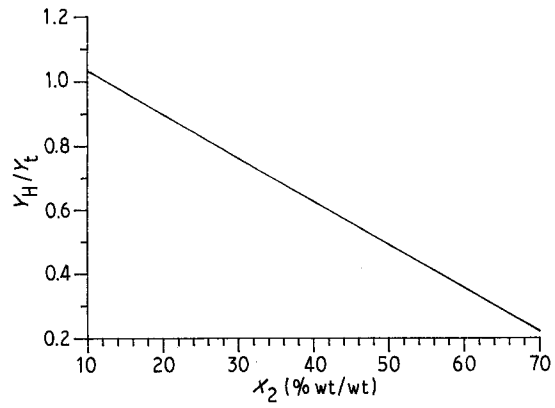

Figure 2 Sorbed water to sorbed toluene volume ratio (Y_H/Y_t) versus polymer surface concentration (X_2, % wt/wt) calculated from the equations of Table V at $EW_i = 0$ and $X_1 = 10\%$ wt/wt.

polymer surface concentration on the Y_H/Y_t ratio, calculated by the use of the constants in Table V.

For ASB–SPPS, diffusion of water through the surface phase is expected due to the presence of the hydrophilic sulphonic functions. Indeed, these materials absorb more water than that expected on the basis of the concentration parameters only. Fig. 3 reports the increase of water sorption (ΔY_H) predicted by the EW terms (i.e. ΔY_H is obtained, for each X-EW experimental set of values in Table I and from Equation 2–III, by calculating the corresponding Y_H value and by subtracting from it the value calculated for the same X values, but for $EW = 0$). It can be observed that at $X_1 < 21$ there is no appreciable effect of the membrane acidity on water sorption although, for these membranes, the acidity values (0.11–0.55 meq g^{-1}) cover almost the entire EW experimental range (extending up to 0.64 meq g^{-1}). At $X_1 > 21$, the acidity effect on water sorption is felt significantly ($\Delta Y_H > \sigma_{ex}$), more and more as the polymer concentration increases and porosity decreases. Fig. 4 shows that, at about the concentration at which ΔY_H is significantly more than zero, the largest pores which are visible on the surface have a diameter of 11 μm, whereas in the bulk phase there are pores as large as 130 μm. By comparison, the largest pores in uncoated asbestos have been shown [7] to be 58 μm on the surface and 200–300 μm in the bulk phase. The pore size of the former composite therefore seems to be that at which the contribution of chemical interaction between the membrane and the external environment becomes appreciable relative to the total liquid sorption. At this pore size, the presence of sulphonic functions within a range of EW values also determines a loss of liquid sorption selectivity by the membrane. The plot (Fig. 5) of the experimental Y_H/Y_t ratio for the acid membranes shows that this loss of selectivity begins to be appreciated at $X_1 > 21\%$. The plot obviously shows that the bulk polymer concentration is not the only parameter to determine selectivity. Fig. 6 shows the effect of the membrane acidity on the calculated Y_H/Y_t ratio for the membrane with porous bulk phase ($X_1 = 10\%$) and non-porous surface ($X_2 = 70\%$), which at $EW = 0$ has been shown to exhibit relatively high toluene sorption selectivity (Fig. 2). The lower selectivity of the acid membrane is explained by the fact that the coating polymer is made by a hydrocarbon lipophilic chain with pendent hydrophilic functions and can allow, within a certain range of EW values, diffusion of the polar and of the non-polar liquid. Extrapolation of the plot in Fig. 6, out of the experimental range, indicates, however, that a selective absorption of water relative to toluene is possible at high membrane acidity.

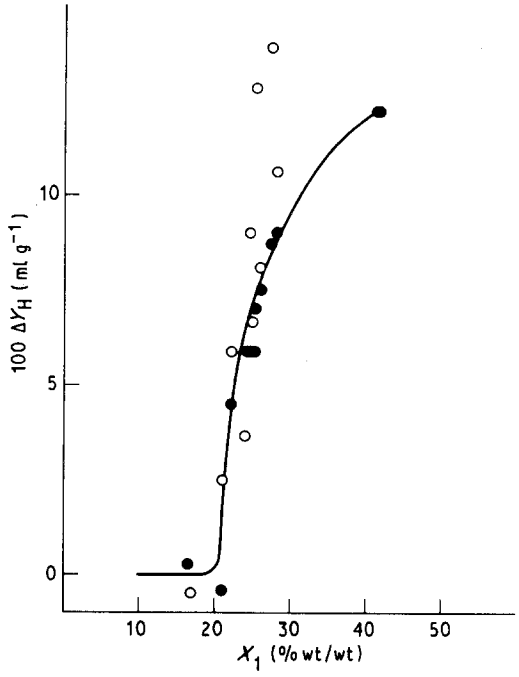

Figure 3 Increase of water sorption (ΔY_H, ml g^{-1}), due to the membrane acidity, for the fresh composites of Table I: (●) ($\Delta Y_H = Y_{Hcld} - Y_{Hcld(EW=0)}$, Y_{Hcld} calculated from Equations 2–III for the X-EW experimental values set in Table I, $Y_{Hcld(EW=0)}$ calculated as above for $EW_i = 0$); (○) ($\Delta Y_H = Y_{Hexp} - Y_{Hcld(EW=0)}$, Y_{Hexp} = experimental value in Table I).

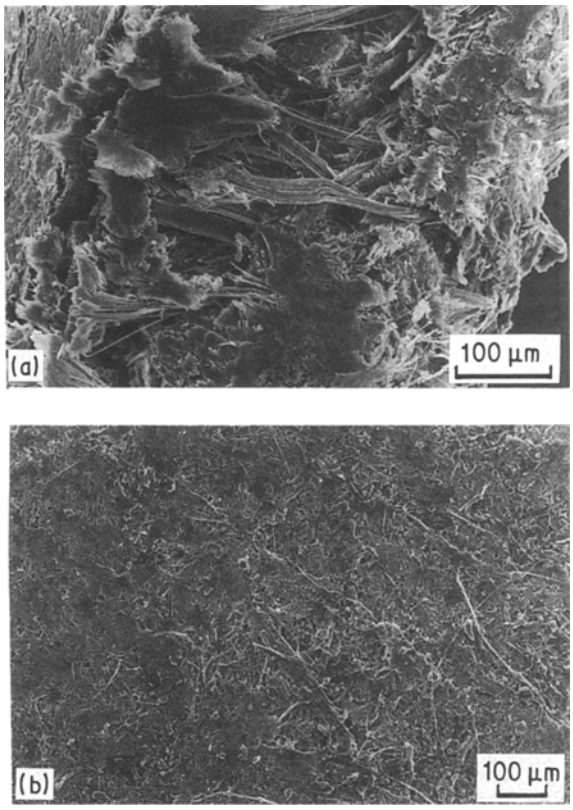

Figure 4 Scanning electron micrograph of fresh ASB–PPS (a) bulk (X_1 = 22.2% wt/wt) and (b) surface (X_2 = 36.7% wt/wt) phase.

For the aged materials (Table II), none of the models in Tables III and IV accounts fully for the change of liquid sorption in excess of the experimental variance. The results of the linear regression analysis (not given), showed that although the correlation coefficient and the parameter's significance levels are high, MSE is significantly $> \sigma_{ex}^2$. The reason for the excess variance probably lies in the fact that, due to the changes brought about by the chemical degradation in the aged material, the independent variables (X and EW) in the above models do not represent the physical and chemical structure of the composite as well as in the fresh material. For the aged materials, the membrane porosity and, therefore the physisorbed

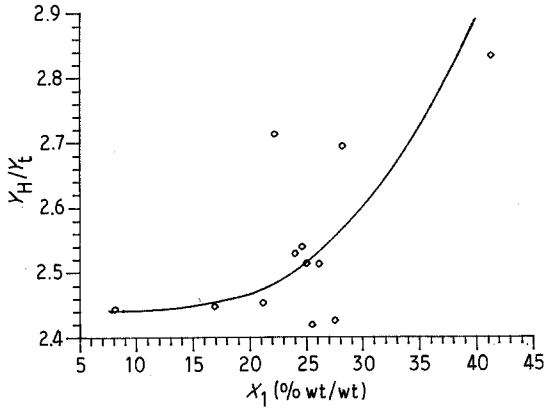

Figure 5 Sorbed water to sorbed toluene volume ratio (Y_H/Y_t = average values of duplicates in Table I) for fresh ASB membranes coated with variable concentration (X_1, % wt/wt) of SPPS.

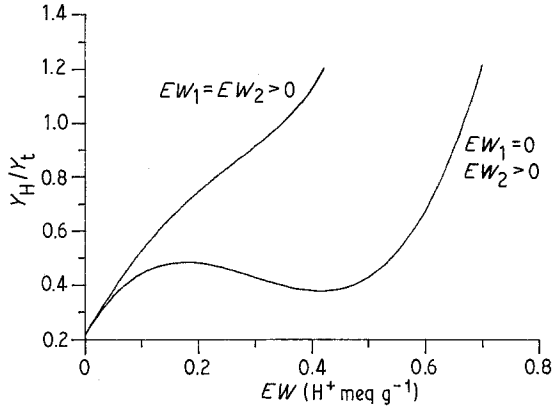

Figure 6 Sorbed water to sorbed toluene volume ratio (Y_H/Y_t) versus membrane acidity calculated from the equations in Table V at $X_1 = 10\%$, $X_2 = 70\%$ and at $EW_1 = 0$, $EW_2 > 0$ or at $EW_1 = EW_2 > 0$.

volume (Y_{pha}) may tentatively be assumed to be related to the volume in the fresh material (Y_{ph}) as in

$$Y_{pha} = Y_{ph} + atwl \quad (12)$$

where Y_{ph} is given by V_0, X_1 and X_2 in the fresh material as in Equation 4 and $atwl$ represents the additional porosity created by weight loss. For the calculation of the chemisorbed volume (Y_{cha}), it must be considered that the aged material contains a new component, brucite, which may interact with the permeant liquid. Y_{cha} therefore may be assumed to be given by

$$Y_{cha} = (s_1 X_{1a} + s_1 X_{2a} + s_2 X_3 + s_4 X_4)/100 \quad (13)$$

where s_1 and s_2 are the specific solubilities in the polymer and in the brucite phase, X_{1a} and X_{2a} are the polymer concentrations in the aged material and X_3 and X_4 are the bulk and surface brucite concentrations. An independent measurement of total porosity would provide a direct estimate of Y_{pha} to fit into a model containing Y_{cha} as a function of the concentration parameters in the aged samples. This additional experimental work, however, was felt unnecessary for the scope of this investigation.

3.3. Behaviour in strong aqueous alkali

The data in Table II require further comment, relevant for the application of asbestos in some major industrial electrochemical processes. The research on asbestos composite cell separators has been aimed at improving the material's chemical stability and at maintaining, at the same time, a good electrical conductivity in the separator phase. For the materials in Table I, Fig. 7 reports the specific conductivity, σ, measured in 30% KOH at 30 °C. The superior performance of the hydrophilic ASB–SPPS separators, over that of ASB–PPS at equal polymer concentration, is clear. Table II, however, shows the opposite order for the chemical stability. It may be observed that, whereas for the ASB–PPS material the weight loss is contained within 14% and seems to decrease for the more concentrated PPS materials, for ASB–SPPS it ranges from 13.9%–37.6% regardless of the polymer concentration. In the light of the results obtained in the liquid sorption study, this behaviour suggests that water chemisorption in ASB–SPPS not only occurs on the polymer membrane surface layer to allow macrodiffusion of the liquid phase into the membrane bulk phase, but also that micro-diffusion within the single asbestos fibre occurs because of the chemical exchange of the alkali between the polymer coating layer and the supporting asbestos fibre. This result reveals that the attainment of low electrical resistance through the use of hydrophilic coating materials is not compatible with securing protection of the asbestos fibres from chemical attack by the alkali.

4. Conclusion

It has been shown that the properties of asbestos in its composites with organic polymers depend on the nature and concentration of the organic polymer. Liquid sorption by these materials occurs by physi-

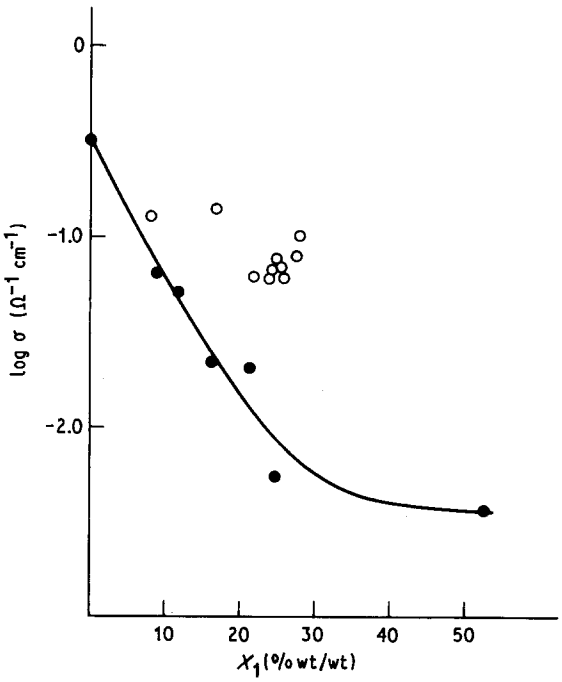

Figure 7 Specific conductivity (log σ, $\Omega^{-1}\,cm^{-1}$), in 30 °C 30% KOH, of (●) ASB–PPS and (○) ASB–SPPS membranes at variable polymer concentration (X_1, % wt/wt).

sorption and/or by chemisorption, depending on the degree of porosity of the solid phase. A mathematical modelling approach, based on a theoretical rationalization of the sorption mechanism, has been used to fit experimental data. The results have shown the importance of the membrane surface phase in determining liquid sorption selectivity and suggest that the membrane surface acidity may be tailored for the separation of molecules which differ in polarity.

For applications in strong corrosive aqueous systems, the membrane acidity is necessary to improve the chemical–physical properties such as the ion transport through a non-porous solid phase. However, in the specific case of alkali-unstable asbestos, it is shown that hydrophilic coating also allows micro-permeation of the alkali through the coated fibre and, consequently, the chemical degradation of the support component. For high-temperature water electrolysis, a porous ASB–PPS material, which works by physisorption only, has been established [10] as a better choice.

Acknowledgement

This work has been partly sponsored by "Progetto Finalizzato del CNR Chimica Fine".

References

1. E. MONTONERI, L. GIUFFRÉ, G. MODICA and E. TEMPESTI, *Int. J. Hydrogen Energy* **11** (1986) 233.
2. E. MONTONERI, G. MODICA and S. MAFFI, *J. Compos. Mater.* **20** (1986) 503.
3. P. GALLONE, "Trattato di Ingegneria Chimica" (Tamburini, Milan, 1973).
4. M. O. COULTER, "Modern Chlor-Alkali Technology" (Ellis Horwood, Chichester, 1980).
5. E. MONTONERI, E. RANZI, G. MODICA and H. HOFMANN, *J. Compos. Mater.* **21** (1987) 690.
6. E. MONTONERI, G. MODICA, L. GIUFFRÉ, L. PERALDO BICELLI and S. MAFFI, *Int. J. Polym. Mater.* **11** (1987) 263.
7. E. MONTONERI, L. GIUFFRÉ, E. TEMPESTI, S. MAFFI and G. MODICA, *Int. J. Hydrogen Energy* **9** (1984) 571.
8. N. R. DRAPER and H. SMITH, "Applied Regression Analysis" (Wiley, New York, 1986).
9. G. BUZZI, FERRARIS, "Analisi ed Identificazione di Modelli", ENI-Ente Nazionale Idrocarburi, Servizio Formazione e Sviluppo, San Donato, Milano (1974).
10. E. MONTONERI, G. MODICA, C. BOWEN, D. GAUTHIER and R. RENAUD, *Int. J. Hydrogen Energy* **12** (1987) 831.

Received 4 September
and accepted 1 December 1989